ChemComm

FEATURE ARTICLE

View Article Online
View Journal | View Issue

Cite this: *Chem. Commun.*, 2016, **52**, 10938

Design directed self-assembly of donor–acceptor polymers

Tomasz Marszalek,[a] Mengmeng Li[a] and Wojciech Pisula*[ab]

Donor–acceptor polymers with an alternating array of donor and acceptor moieties have gained particular attention during recent years as active components of organic electronics. By implementation of suitable subunits within the conjugated backbone, these polymers can be made either electron-deficient or -rich. Additionally, their band gap and light absorption can be precisely tuned for improved light-harvesting in solar cells. On the other hand, the polymer design can also be modified to encode the desired supramolecular self-assembly in the solid-state that is essential for an unhindered transport of charge carriers. This review focuses on three major factors playing a role in the assembly of donor–acceptor polymers on surfaces which are (1) nature, geometry and substitution position of solubilizing alkyl side chains, (2) shape of the conjugated polymer defined by the backbone curvature, and (3) molecular weight which determines the conjugation length of the polymer. These factors adjust the fine balance between attractive and repulsive forces and ensure a close polymer packing important for an efficient charge hopping between neighboring chains. On the microscopic scale, an appropriate domain formation with a low density of structural defects in the solution deposited thin film is crucial for the charge transport. The charge carrier transport through such thin films is characterized by field-effect transistors as basic electronic elements.

Received 30th May 2016,
Accepted 7th July 2016

DOI: 10.1039/c6cc04523e

www.rsc.org/chemcomm

1. Introduction

Organic electronics have found the way from basic academic research to industrial applications over recent years in a quickly growing market. This market covers especially application fields

[a] *Max Planck Institute for Polymer Research, Ackermannweg 10, 55128 Mainz, Germany. E-mail: pisula@mpip-mainz.mpg.de*
[b] *Department of Molecular Physics, Faculty of Chemistry, Lodz University of Technology, Zeromskiego 116, 90-924 Lodz, Poland*

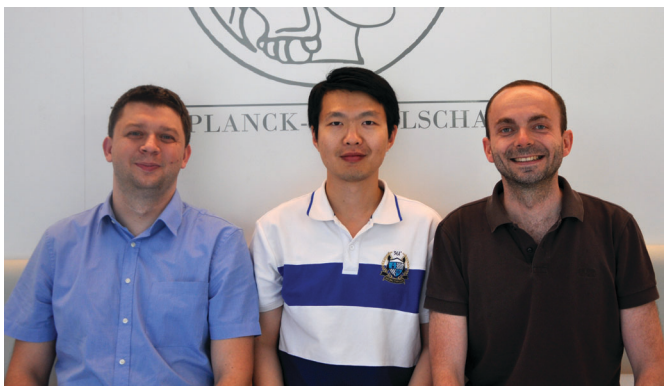

Tomasz Marszalek (left), Mengmeng Li (middle) and Wojciech Pisula (right)

Tomasz Marszalek has been a postdoctoral researcher in the Group of Professor Klaus Müllen at Max Planck Institute for Polymer Research since 2012. He completed his PhD under the supervision of Professor Jacek Ulanski in the Department of Molecular Physics at Lodz University of Technology. His research interests lie in the field of organic electronics and self-assembly of low and high molecular weight organic semiconductors.

Mengmeng Li obtained his PhD degree under the supervision of Professor Klaus Müllen at the department of synthetic chemistry of the Max Planck Institute for Polymer Research in Mainz in 2016. His main research interests include self-assembly control of organic semiconductors in field-effect transistors and other related electronic devices.

Wojciech Pisula studied chemical engineering at the University of Applied Science Osnabrück and at the University of Wales, Swansea, where he gained his Master of Science. In 2001, he joined the group of Professor Klaus Müllen at the Max Planck Institute for Polymer Research, where he completed his dissertation in 2005. In 2006 he changed to a full position at Evonik Industries AG keeping at the same time his status as project leader at the MPIP. At the beginning of 2015 he received his habilitation in material science at the Technical University of Darmstadt under the mentorship of Professor Heinz von Seggern. Since mid 2015 he has been additionally employed as an associate professor at the Lodz University of Technology in the Department of Molecular Physics of Professor Jacek Ulanski. Wojciech's research interests are physical chemical aspects of π-conjugated self-organizing systems and the resulting functionalities.

in light emitting diodes (LEDs),[1,2] field-effect transistors (FETs)[3,4] and solar cells[5] which open the window for novel technologies. Organic semiconductors consist of conjugated molecules which can be processed into devices from solution, allowing a large surface-area.[6,7] Moreover, many active compounds are mechanically flexible and therefore applicable to bendable electronic elements.[8] Due to the low cost processing, one-way applications of electronic elements are realizable like radio frequency identification (RFID) tags and sensors in which FETs play a major role.[9,10] The performance of a transistor is mainly determined by the speed of the charge carrier transport from one electrode to the other which in turn depends on various factors related to the semiconducting system which are discussed in the next paragraph in more detail.[11–13]

Organic semiconductors can consist of either small conjugated molecules or long polymers. In both cases, the π-conjugated bonds lead to delocalized filled and empty π-orbitals which affect the electrical and optical behavior of the semiconductor.[14] The (macro)molecules weakly interact in solution and solid-state by π-stacking, van der Waals or dipole–dipole forces leading to so-called self-assembly into distinct aggregates and superstructures.[15] This self-assembly of the polymer at the nano- and mesoscale determines the transport of charge carries through the active layer.[16–18] Small molecules and polymers differ significantly in their assembly and transport properties. The first type of system shows a pronounced tendency to strongly crystallize leading to a high degree of (long-range) order and close π-stacking, defined here as packing. However, small molecules suffer from inhomogeneous film formation and create distinct grain boundaries as effective charge carrier traps due to their high crystallinity. Their additional apparent electronic anisotropy makes an implementation into large transistor arrays challenging. In contrast, conjugated polymers organize in layer structures that are less sensitive to the relative lattice orientation towards the transport direction.[19] It is assumed that a fast charge carrier migration takes place along the conjugated backbone, while hopping of charges occurs between polymer chains preferentially along the π-stacking direction. When deposited on the device surface from solution, macromolecular semiconductors organize into complex and hierarchical superstructures over different length scales.[20] A high performance device requires an optimization over a wide range from a few Å to several micrometers which is critical for the device. The above mentioned local packing in the range of a few Å to a few nm within a periodic lattice is dictated by the polymer design and chemistry and thus by intermolecular interactions. Locally, the relative polymer backbone arrangement has impact on the π-orbital overlap of neighboring chains and affects the charge hopping. In contrast to small crystalline molecules, conjugated polymers reveal also micrometer large areas of varying order leading to so-called semicrystalline microstructures with separated regions of both high crystallinity and disorder (amorphous). It is assumed that in polymers with ultrahigh charge carrier mobilities the ordered domains are interconnected by loose polymer chains that ensure a charge transfer.[21] The nucleation and growth during the self-assembly process into corresponding structures is governed also by the polymer intermolecular interactions. At a meso- and macroscopic scale, crystallite size and texture become relevant structural parameters for the charge carrier transport. Long-range order, large domain size as well as crystallite orientation with respect to neighboring domains and transport direction favor the conduction in the device.[22] Disordered regions and pronounced grain boundaries between small domains limit the performance of a transistor. Additionally, the polymer orientation with respect to the surface is another important factor for the device operation. The backbones can arrange either in a face- or edge-on fashion on the substrate. In an edge-on organization, the aromatic plane is normal to the surface so that the π-stacking axis is oriented parallel to the substrate. This orientation is required for application in transistors where the transport occurs also parallel to the surface close to the dielectric/semiconductor interface.

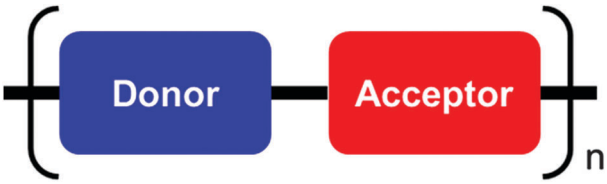

Fig. 1 General structure of a simplest D–A polymer backbone consisting of an electron deficient and an electron rich unit. D–A polymers can also comprise more units within one monomeric building block.

For a long time the charge carrier mobilities in polymer transistors have been generally low due to the poor packing and lack of macroscopic order of these materials.[23] There have been several approaches towards enforcing thin film crystallinity in order to solve this problem.[24] In contrast to homopolymers, donor–acceptor (D–A) copolymers consist of an alternating arrangement of units of different electron affinity and are considered as rigid-rod macromolecules (Fig. 1).[25] The low band gap of such polymeric systems makes them attractive for applications in organic photovoltaic cells.[26,27] Moreover, in many cases the planar arrangement of the conjugated backbone ensures a close π-stacking distance which is relevant for efficient intermolecular charge carrier transport.[28] A close packing of the polymer chains might be favored from additional donor–acceptor interactions.

This review discusses the role of the macromolecular structure of D–A copolymers on their local packing, supramolecular organization, and microstructure formation. Understanding the interplay between macromolecular design, organization of the polymer within nano- and microscopic dimensions as well as charge carrier transport opens the door towards the development of new polymeric semiconductors of superior performance for future applications. The structure variety in the discussed D–A polymers contains a broad toolbox of crucial structural features including molecular weight, bulkiness and substitution position of the alkyl chains and backbone curvature.

2. General features of donor–acceptor polymers

As said before, the backbone of this polymer type is built on one or more electron donors and electron acceptors (Fig. 1).

The modification of the electron pushing and pulling strength of the units allows controlling of the highest occupied molecular orbital (HOMO) and lowest unoccupied molecular orbital (LUMO) energy levels of the polymer. This is possible since the HOMO is mainly sited at the donor unit, while the LUMO is related to the acceptor. Consequently, the band gap can be reduced to even around 1 eV.[29] This low value makes D–A polymers attractive for solar cell applications due to an increase of the absorption over a broad wavelength range. Recently, D–A polymers revealed in heterojunction solar cells in combination with fullerenes power conversion efficiencies up to 10%.[30] The extended intrachain conjugation and intense donor–acceptor interactions *via* electron transfer lead to a small torsion angle favoring tight π-stacking packing of the polymer chains in the layer structure and high crystallinity. Consequently, D–A polymers with these characteristics show record mobilities in FETs far beyond 5 $cm^2 V^{-1} s^{-1}$ for holes and electrons.[31,32] The intralayer stacking of the D–A polymers can be determined by either solid-state nuclear magnetic resonance (NMR) or electron diffraction. It was proven by a combination of solid-state NMR and X-ray diffraction (XRD) that the hexadecane substituted cyclopentadithiophene–benzothiadiazole polymer **2a** is π-stacked in a lamellar kind of fashion with donor and acceptor units ordered in an alternating way (Fig. 2a).[33]

In this model, the acceptor groups in adjacent layers are located on top of each other. This seems to be an optimal polymer packing for **2a** as the long hexadecane side chains avoid steric clash. For another type of D–A polymer, a naphthalene–diimide–bithiophene polymer **1**, two distinct polymorphs have been found in oriented

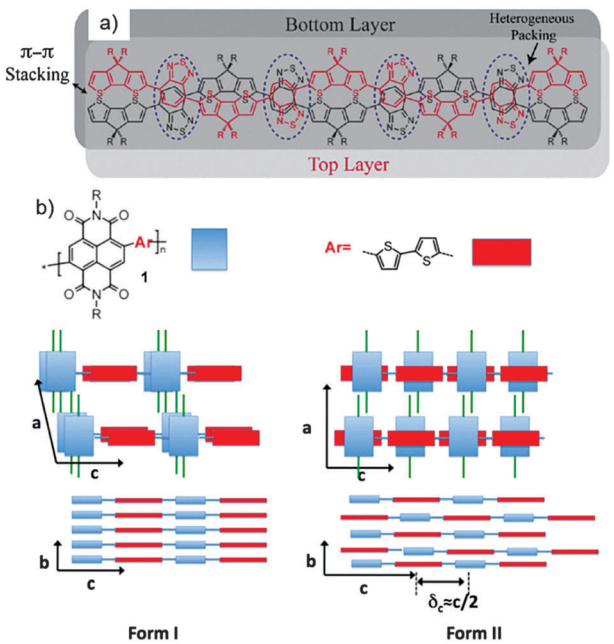

Fig. 2 Schematic drawing illustrating the local packing of donor–acceptor groups in two neighboring polymer chains of (a) **2a** (blue dashed circles mark regions where the acceptor groups are heterogeneously packed on top of one another) and (b) of **1** with NDI and T2 units in forms I and II. In form I, NDI and T2 units are forming segregated columns, while in II, the units are in π-overlap one with another. Reprinted with permission from ref. 33 and 34, Copyright 2011 and 2012, American Chemical Society.

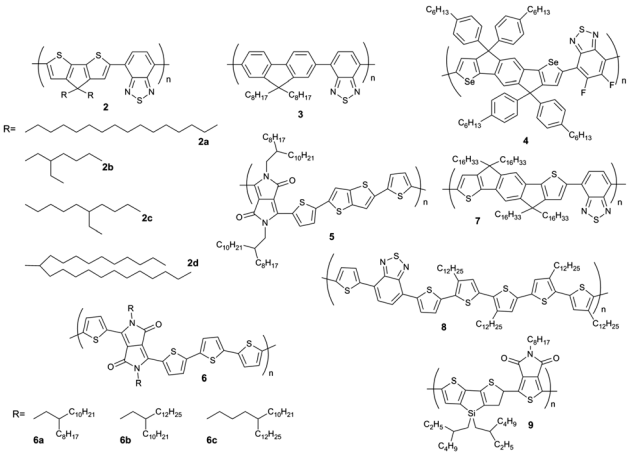

Fig. 3 Chemical structures of D–A polymers chosen to describe the influence of molecular weight on charge carrier mobility.

films depending on the underlining substrate.[34] During directional epitaxial crystallization from 1,3,5-trichlorobenzene polymer **1** organizes in segregated columns of bithiophene (2T) and naphthalene diimide (NDI) units leading to form I (Fig. 2b). On poly(tetrafluoroethylene) (PTFE) substrates form II is obtained after cooling the film from the melt with *c*/2 shifted neighboring backbones so that NDI and T2 units are in π-overlap one with another (Fig. 2b). Form I can be transferred to form II by annealing at a temperature above 250 °C. Due to different π-stacking modes of NDI and T2, the two polymorphs show characteristic signatures in the UV-vis spectra. A similar change in packing mode was reported in spin-coated poly(octylfluorene-*alt*-benzothiadiazole) (**3**) films of high molecular weight (Fig. 3).[35] The columnar type of segregated packing was related to the large torsion angle between the F8 and BT units decreasing the distance between neighboring chains.

3. Molecular weight

The molecular weight of D–A copolymers plays a critical role for their charge carrier transport. Fig. 4 summarizes the field-effect mobilities of several D–A polymers as a function of number average molecular weight M_n neglecting the polydispersity for simplification. A general trend can be identified with thin films of higher M_n polymers exhibiting larger mobilities. For instance, with doubling M_n from 30.1 to 61.8 kg mol^{-1}, the average hole mobility of **4** (Fig. 3) can be enhanced by two orders of magnitude from 2×10^{-3} to 0.15 $cm^2 V^{-1} s^{-1}$.[39] A 10-fold improvement in hole transport for **2** has been also observed when increasing M_n from 11 to 35 kg mol^{-1} yielding a maximum mobility of 3.3 $cm^2 V^{-1} s^{-1}$.[33] In the case of a DPP–DTT polymer **5**, ultrahigh molecular weight has been achieved with M_n = 110 kg mol^{-1} resulting in an extremely high mobility with an average of 8 $cm^2 V^{-1} s^{-1}$ and maximum of 10.5 $cm^2 V^{-1} s^{-1}$. On the contrary, the low molecular weight **5** (M_n = 29 kg mol^{-1}) shows a much poorer transistor performance with a mobility of about 1 $cm^2 V^{-1} s^{-1}$.[44]

One explanation for the M_n dependent mobility is that ordered regions in films are more densely interconnected by

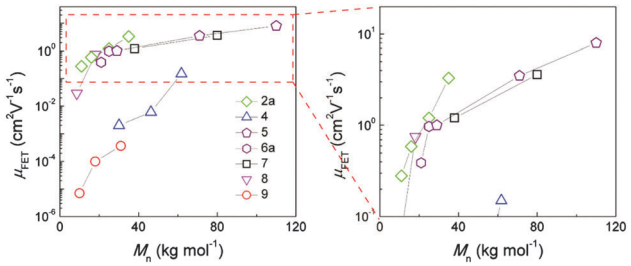

Fig. 4 Dependence of field-effect mobility of D–A polymers on molecular weight.[36–43]

longer polymer chains facilitating charge carrier transport though the disordered regions.[40] This model is based on the assumption that the polymers which lack such a network ultimately result in a lower transistor performance. Another proposed mechanism is related to the polymer ordering. For CDT–BTZ polymers (**2**) it has been found that the film microstructure is independent of the molecular weight, but the crystallinity is significantly improved for higher M_n as evident from XRD data.[33] As shown in Fig. 5a, the XRD diffraction peak for the highest M_n (35 kg mol^{-1}, blue plots) is narrower than for polymers with lower M_n indicating higher crystallinity and a more pronounced polymer order for the first case. Additionally, the interlayer distance between backbones decreases from 2.78 nm for M_n = 11 kg mol^{-1} to 2.56 nm for M_n = 35 kg mol^{-1}. A high order and tighter packing favor the charge carrier transport leading to a maximum value of 3.3 cm^2 V^{-1} s^{-1} for M_n = 35 kg mol^{-1}. An identical trend has been observed for **5** as shown in Fig. 5b. The XRD diffraction intensity is enhanced with increasing molecular weight suggesting an increased crystallinity of the thin films.[44] This increase in crystallinity is in good agreement with the M_n dependent mobility (Fig. 4).

However, some exceptions exist in which the molecular weight has no or negative impact on the charge carrier transport. In spite of improved molecular ordering with higher M_n, a quinacridone-based D–A polymer exhibited an M_n independent behavior of charge carrier transport in M_n ranges from 12 to 46 kg mol^{-1}.[45] Another unusual example is the n-type D–A polymer **1**. It has been found that the low molecular weight derivative shows a superior electron mobility in comparison to the high molecular weight one, which is attributed to its higher crystallinity.[46]

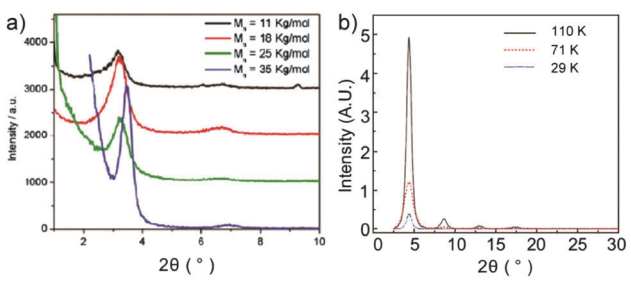

Fig. 5 X-ray diffraction of D–A polymer thin films of different molecular weights for (a) **2a**[33] (reprinted with permission from ref. 33, Copyright 2011, American Chemical Society) and (b) **5**[43] (reprinted with permission from ref. 43, Copyright 2012, Nature Publishing Group).

4. Side chain engineering

As is mentioned in the previous sections, the device performance is typically strongly connected to the order of D–A polymers. Further aspects like supramolecular organization, local packing and microstructure formation are also important for the charge carrier transport and are determined mainly by the self-assembly propensity of the polymer and thus by intermolecular interactions. Due to these forces, the polymers can arrange into a three dimensional organization with long-range order which is necessary for an unhindered charge transport through the active layer. As a drawback, strong interactions between polymer chains can significantly reduce the solubility of these materials. To control the solubility and allow deposition of the polymers from solution, alkyl side chains are attached to the rigid backbone. Depending on the geometry of these substituents, the polymer interactions can be well controlled.[47] Side chains also fulfill another important function. They take an essential role during the self-assembly of the polymer chains into distinct supramolecular structures. Typically, linear alkyl chains tend to form interchain interdigitation which promotes the formation of well-defined layered structures and increases the crystallinity as mainly proven for poly(alkylthiophenes).[48] It is generally assumed that a highly crystalline layer structure favors the charge carrier transport. Interestingly, some D–A polymers revealed a contrary behavior.[21]

4.1. Linear *vs.* branched alkyl chains

To ensure sufficiently high solubility for device fabrication and good film formation of the rigid polymers branched side chains are usually chosen. Due to their higher steric hindrance these substituents lower the polymer interactions, can decrease the polymer planarity and rise the π-stacking distance within the layer structure.[49] The π-stacking distance can therefore increase even by 0.5 Å significantly reducing the hopping rate of the charge carriers along the packing direction. Simulations have indicated that the electronic couplings decay exponentially with the stacking distance for cofacially π–π packed model systems and can vary even by a factor of 4 for an increase in packing distance of 0.5 Å.[50] The relation between alkyl substituents and molecular organization has been discussed for CDT–BTZ polymers (**2**) for which the π-stacking distance increases from 3.5 Å to 4.0 Å by replacing the linear hexadecane alkyls (**2a**) by long branched decyl-tetradecyl ones (**2d**).[51] In the case of **2d**, the long branched decyl-tetradecyl chains surprisingly crystallize in the layer periphery inducing a pronounced microstructure in comparison with **2b** with shorter branched ones. Due to the large π-stacking distance of 4.0 Å, the charge carrier mobility of **2b** and **2d** in FETs drops by several orders of magnitude in comparison to **2a**. Interestingly, at the same time both polymers reveal an ambipolar behavior. This change in device operation in contrast to hole transporting **2a** is related to a lateral shift of the backbones towards each other by 1–1.5 Å provoked by the high steric hindrance of the branched alkyl chains as indicated by solid-state NMR. Simulations have proven that this lateral shift equals the transfer integrals for

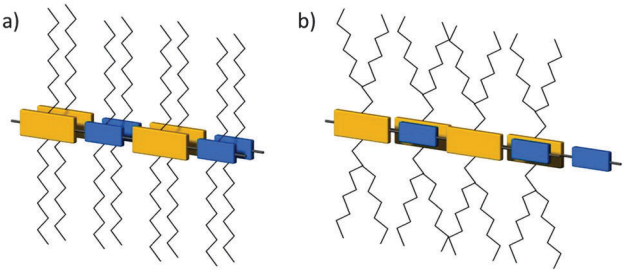

Fig. 6 Schematic illustration of polymers with (a) alkyl chains attached to donor and acceptor units, (b) molecular docking with substituents attached only to one donor or acceptor unit.

holes and electrons on the same level from an initially hole dominated value of **2a**.[52] Besides the increase in stacking distance and backbone shift, the implementation of branched side chains can reduce the coherence lengths for the π-stacking and layer structure as a direct consequence of the lower backbone planarity.[53] This in turn decreases the overall crystallinity that is crucial for the charge migration.

Another concept to tune the packing is based on "molecular docking" of isoindigo polymers **28** (Fig. 18) in which the spatial steric hindrance caused by branched alkyl chains is reduced by removal of these substituents just from the small units (Fig. 6).[54] Following this approach, the smaller units dock into the cavity of the larger one accompanied by an improvement of the interchain π-stacking and carrier mobility. The packing is further enhanced by using centrosymmetric donor units yielding linear rather than curved backbone conformations (see further discussion on curvature in Section 5).

The side chain toolbox with linear, branched and hybrid substituents is also powerful to fine control the surface arrangement of the D–A polymers (Fig. 7). Besides the variation between edge-on and face-on[55] the surface orientation can also include intermediate isotropic or bimodal states in active films (Fig. 7c). The backbone organization on the surface has tremendous impact on the charge carrier transport in the device. Charge transport in polymer films generally contains intrachain and interchain processes. The intrachain conduction is realized by π-electron delocalization along polymer backbones, providing high carrier mobility. This process is largely determined by the effective conjugation length of the polymer, which is limited by the torsional disorder along the backbone and the presence of chemical defects.[56] The interchain transport is generally classified as a hopping mechanism. The most effective transport in transistors is achieved in the case of the edge-on organization with the π-stacking oriented parallel to the substrate and in the

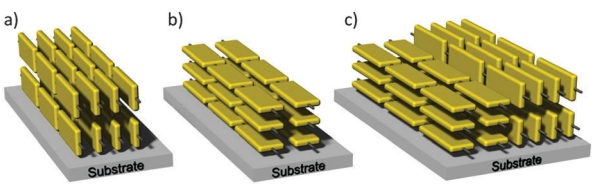

Fig. 7 Motifs of the polymer orientation on surfaces with (a) edge-on, (b) face-on, (c) bimodal arrangement.

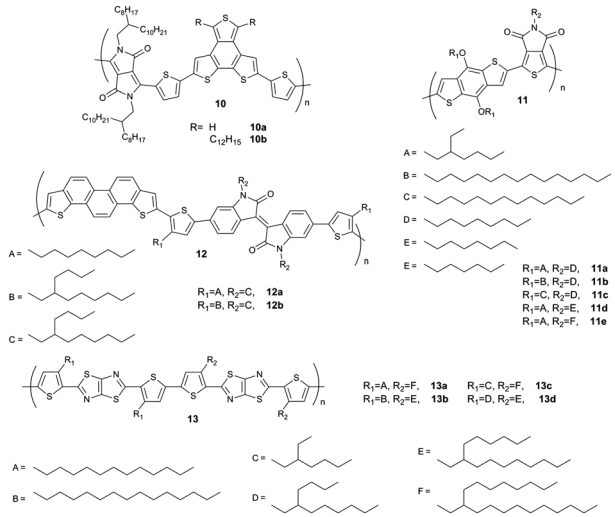

Fig. 8 Chemical structures of D–A polymers with linear and branched alkyl substituents.

same plane of the charge transport. In a face-on organization the aromatic plane of the backbones lies flat on the surface so that the π-stacking is perpendicular to the substrate. This arrangement is beneficial in diode-like devices in a top and bottom electrode architecture as such heterojunction solar cells. The heterojunction morphology is typically formed from a mixture of a D–A polymer as donor system and a functionalized fullerene derivative as acceptor. The faster the holes and electrons are transported to the corresponding electrodes after exciton separation, the smaller the probability of recombination and finally the higher the solar cell efficiency. The conduction in diodes takes place out-of-plane to the surface which is in agreement with the π-stacking direction in a face-on organization.

It has been shown for D–A polymers based on diketopyrrolopyrrole (**10**),[57] thienopyrroledione (**11**)[58] or phenanthrodithiophene–isoindigo (**12**)[59] (Fig. 8) that bulky and sterically demanding side chains result in a face-on arrangement, while edge-on is triggered by linear ones in drop-cast and spin-coated films (Fig. 9). These changes in backbone orientation on the substrate are directly correlated to the device performance in transistors or solar cells. The mechanism in surface orientation is attributed to the polymer aggregation in solution before deposition. Strongly interacting polymer chains with linear substituents result in aggregates in solution which arrange edge-on on the surface. Upon poor aggregation single polymer chains present in the solution are flexible and capable to interact with the surface *via* van der Waals ordering in the face-on fashion. For polymer **13** the backbone orientation is altered through fine-tuning of the length difference between two alkyl substituents.[60] For an edge-on orientation of **13**, the length difference between the linear and branched side chain has to be large like in **13b** and **13c**. When the length difference is small, such as in **13a** and **13d**, the macromolecules tend to form a well-ordered face-on assembly. Bulk heterojunction solar cells reveal the highest short-circuit current density for films with primarily face-on orientation.

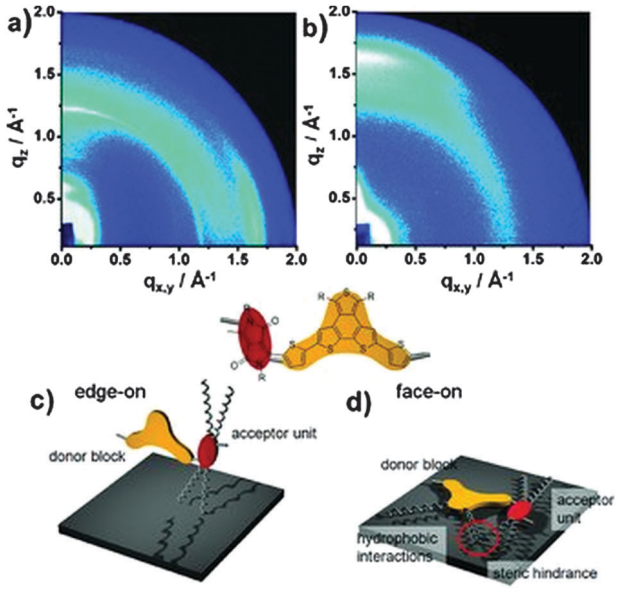

Fig. 9 GIWAXS patterns of (a) **10a** and (b) **10b**, schematic illustration for one repeating unit in a (c) edge-on for **10a** and (d) face-on for **10b** orientation towards the HMDS modified surface. The red circular areas indicate the steric hindrance between alkyl chains. Reprinted with permission from ref. 57, Copyright 2013, Wiley-VCH Verlag GmbH.

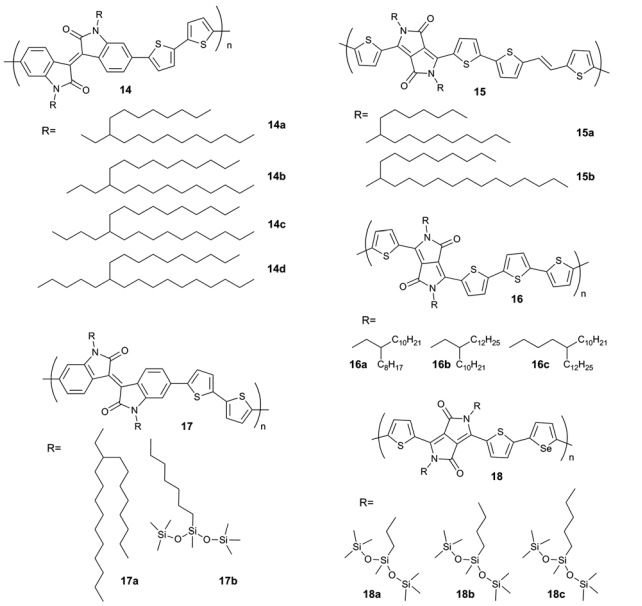

Fig. 10 Chemical structures of D–A polymers chosen to discuss the influence of the branching point and hybrid composition of the substituents.

4.2. Role of bifurcation point

To overcome the steric impact of the branched alkyl substituents on the polymer packing, but to maintain the solubility, one strategy is to shift the branching point away from the backbone. Side chains with a branching point in proximity to the backbone hamper particularly the π-stacking interactions and lower the hopping rate of charge carriers. Systematic studies have shown that the spacer length between the branching point and the backbone plays an important role on polymer packing and transport of charge carriers.[61,62] The reduced steric hindrance of attached alkyls allows closer π-stacking and lowers the polymer twisting leading to a more planar backbone.[63] For instance, the π-stacking distance decreases from 3.75 Å for **14a** to 3.57 Å for **14c** and **14d**, while at the same time the interlayer distance of edge-on oriented polymers increases with longer alkyl chains.

The same concept has been successfully applied for CDT-BTZ polymers (**2**). The 5-ethylnonyl side chains in **2c** result in improved supramolecular organization in comparison to **2b** with 2-ethylhexyls.[64] Significant differences are also evident in the film microstructure. Polymer **2b** possesses a lower solubility leading to the formation of 80 nm to 200 nm large aggregates, while a nanofiber network (diameter of 10 nm and length of about 100 nm) is obtained for **2c**. The mobility for **2c** is more than one order of magnitude higher than for **2b** due to a smaller π-stacking distance and the fiber formation. The transport in **2b** is disturbed by distinct grain boundaries, while nanofibers of **2c** serve as good pathways for charge carriers allowing a 2D migration through the network.

A similar trend has been also observed for DPP polymers. A charge carrier mobility of 8.2 $cm^2 V^{-1} s^{-1}$ has been determined for a polymer with decyltetradecyl substituents (**15a**) which is two times larger than for the derivative with shorter octyldodecyl side chains (**15b**) (Fig. 10).[65] This mobility increase is attributed also to stronger polymer interactions and a smaller π-stacking distance of 0.36 nm for **15a** in comparison to 0.37 nm for **15b**. Apart from the reduced π-stacking distance, the large size and high crystallinity of the domains improve the mobility, as well. The influence of branched alkyl chains and bifurcation point has been also investigated for other DPP-based polymers (**16**).[66] Although the crystallinity of the DPP derivatives **16a** and **16b** (Fig. 10) is similar and the π-stacking distance for **16a** is smaller, **16b** shows a higher charge carrier mobility within the series of **16**. The enhanced performance of **16b** is assigned to its homogenous film and better interconnected network ensuring a more efficient charge transport between grains. Longer alkyl chains in **16c** in comparison to **16b** and **16a** reduces the crystallinity, but increased the charge carrier mobility due to a shorter π-stacking distance. As in the other examples, the lowered π-stacking distance and increasing the backbone planarity are induced by shifting the bifurcation point.

4.3. Inorganic substituents

An identical correlation between branching point and packing has been found for D–A polymers siloxane-terminated substituents. The first approach has been reported for hybrid siloxane-terminated groups attached at an isoindigo-based polymer **17b** ensuring a sufficient solubility for solution processing (Fig. 10).[67] In comparison to a reference polymer **17a** with branched alkyl side chains the π-stacking distance was reduced from 3.76 Å to 3.58 Å due to an enhanced backbone planarity leading to an increase of the hole mobility in transistors from 0.57 $cm^2 V^{-1} s^{-1}$ to 2.48 $cm^2 V^{-1} s^{-1}$. An additional factor responsible for the device improvement was a bimodal edge- and face-on arrangement of **17b** on the surface allowing a 3D charge transport to by-pass structural defects through the active film (Fig. 11).

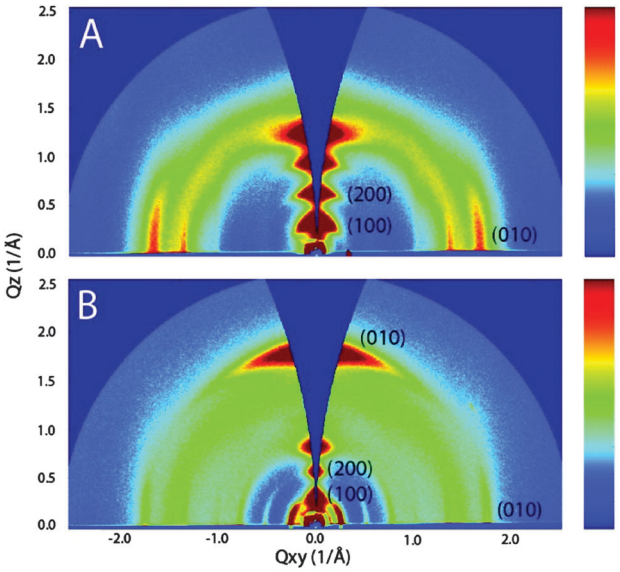

Fig. 11 GIWAXS patterns of **17a** (A) and **17b** (B). Polymer **17a** displays lamellar packing common to many conjugated polymer films, with the π-stacking Bragg planes parallel to the substrate plane. In contrast, **17b** crystallites contain two kinds of textures, where the π-stacking planes are both normal and parallel to the substrate.[67] Reprinted with permission from ref. 67, Copyright 2011, American Chemical Society.

Similar to pure hydrocarbon substituents in **14**, an important role of the spacer length has been found for the hybrid siloxane side chains on the organization and charge transport on transistors. Thereby, the ambipolar performance of DPP–selenophene polymers **18** is optimized by adjusting the branching position of siloxane substituents (Fig. 10). Polymers with reduced spacer length **18a** and **18b** exhibit enhanced charge transport relative to **20c** due to a smaller lamellar spacing and a denser network of fibers in the film (Fig. 12), while retaining a close π-stacking distance.[68] Solution-sheared films of **18b** processed at elevated temperatures show unprecedentedly high hole and electron mobilities of 8.84 $cm^2 V^{-1} s^{-1}$ and 4.34 $cm^2 V^{-1} s^{-1}$, respectively.

4.4. Odd–even effect of substituents

Not only the spacer length, but also its odd–even carbon number has impact on the self-organization and electrical properties of D–A polymers (Fig. 13). Polymer derivatives **19** with branched alkyl groups containing linear spacers from C_2 to C_9 show such an odd–even effect.[69] Alkyl spacers with even numbers of carbon atoms (C_2, C_4, and C_6) exhibit shorter lattice spacing than spacers with odd carbon numbers (C_3 and C_5) resulting in one order of magnitude higher charge mobilities. It is assumed that various torsion angles with respect to the alkyl chain branching position affect the polymer packing resulting in longer/shorter *d*-spacing upon odd/even numbered spacers. The denser packing of **19** with even numbered spacers (C_2, C_4, and C_6) implies that their alkyl side chains might undergo relatively strong interdiffusion reducing the intermolecular spacing of the polymer backbones. As the side chain length increases the odd–even effect fades for lengths larger than C_7. The longer alkyl spacer may shield the odd–even effect for the polymer packing due to their unpredictable interaction with neighboring segments.

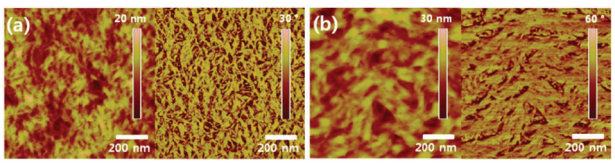

Fig. 12 AFM height (left) and phase (right) images of solution-processed drop-cast films of (a) **18a** and (b) **18b**.[68] Reprinted with permission from ref. 68, Copyright 2013, American Chemical Society.

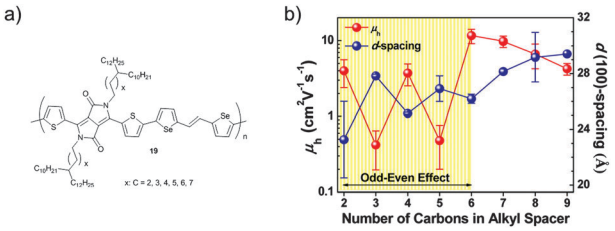

Fig. 13 (a) Chemical structure of **19** revealing an odd–even effect of the alkyl spacer, (b) average mobility and *d*(100)-spacing values of **19** as a function of carbon number in the spacer.[69] Reprinted with permission from ref. 69, Copyright 2015, American Chemical Society.

4.5. Substituent position

Besides the geometry of the side chains, their substitution position at the backbone plays also an important role on the supramolecular organization of D–A polymers. For instance, the variation in alkyl chain orientation at the rigid backbones significantly influences the packing and charge carrier transport of three thienopyrroledione-based polymers **20** with a similar alkyl chain density, but differing in the side chain position (Fig. 14).[70] Polymer **20b** possesses a large space between clusters of alkyl chains and facilitates in this way interdigitation, formation of layer structures and large intermolecular overlap. In contrast, a small space between alkyl clusters and non-uniform chain orientation in **20a** and **20c** hinders interdigitation and intermolecular overlap. For this reason, the mobility of **20c** is more than two orders of magnitude higher in comparison to

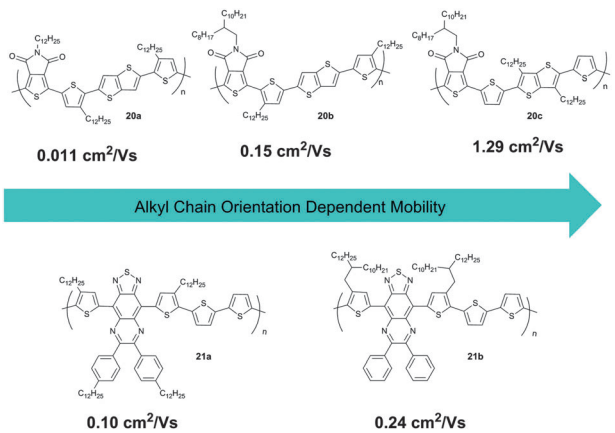

Fig. 14 Relation between charge carrier mobility and alkyl chain position in selected D–A polymers.

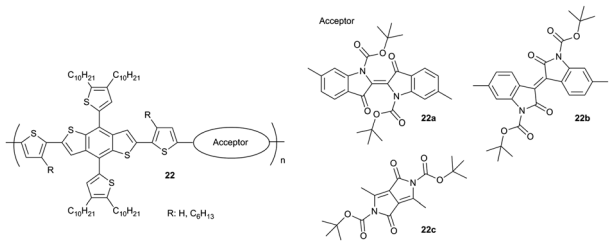

Fig. 15 Chemical structures of D–A polymer with thermally removable substituents.

20a and **20b**. The geometry and localization of linear and branched substituents have been also investigated for thiadiazoloquinoxaline-based polymers **21**. A pair of 2-decyltetradecyl chains in **21b** used to replace the linear side chains in **21a** does not significantly change the planarity of the polymers, but improves the molecular weight and solubility. In this way, the films are more homogenous and show higher crystallinity in the π-stacking direction of the polymer. Therefore, the charge carrier mobility of **21b** increases up to 0.24 $cm^2 V^{-1} s^{-1}$ with respect to **21a** (Fig. 14).

4.6. Thermally controlled substituents

One recent strategy has used thermally removable substituents to turn the polymer film insoluble for subsequent film deposition and to reduce the portion of isolating alkyl chains in the active layer. The main requirement is that the electronic nature of the polymer backbone remains unperturbed by the bond scission. The cleavage mechanism of the substituents has been well described for polythiophenes as model systems[71] and the approach has been recently transferred to a series of narrow band gap D–A polymers comprising *tert*-butoxycarbonyl (*t*-Boc) substituted indigo (**22a**), isoindigo (**22b**) or diketopyrrolopyrrole (**22c**) as the acceptor and benzodithiophene as donor moiety (Fig. 15).[72] Thermal treatment of **22c** films at 200 °C leads to the cleavage of the *t*-Boc side groups along with the formation of a hydrogen-bonding network and enhanced backbone planarity due to a reduction of the steric hindrance. A higher planarity facilitates intermolecular interactions between fused ring moieties and the thiophene segments. For this reason, the interlayer and π-planar distances decrease after thermal reduction being beneficial for the charge carrier transport in transistors (Fig. 16).[73]

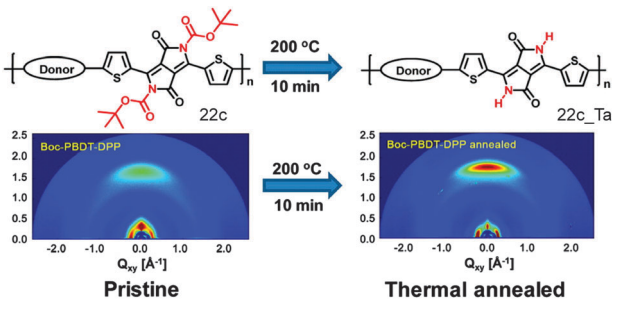

Fig. 16 Schematic illustration of the thermal reduction of the substituents in **22c** and GIWAXS patterns obtained before and after substituent reduction. Reprinted with permission from ref. 72, Copyright 2015, American Chemical Society.

5. Role of backbone curvature

The backbone curvature can significantly impact the supramolecular organization of D–A polymers. For instance, polythiophene derivatives with increased backbone curvature result during synthesis generally in low molecular weight. The effect of molecular weight reduction is attributed to difficulties during polymerization by reducing the accessibility of the reactive chain ends for further reactions. The flexibility of polymers is strongly connected to their solubility which is also affected by the backbone curvature. On the one hand, the polymer solubility is increased with higher backbone curvature resulting in reduced aggregation of the rod-like polymers. On the other hand, a too high curvature hinders lamellar packing due to higher entropy. In the solid-state, an increased interlayer distance is typically observed for more curved polymers since side chains on the bent backbones cannot interdigitate as effectively as in the case of linear polymers.[74] The influence of interdigitation on the organization and charge carrier transport has been already discussed in a previous section.[74] The role of different bonding geometries of dithieno-carbazole-based D–A polymers on the backbone conformation has been studied for a series of derivatives with various donor and acceptor units (**23–25**). Polymers **23a**, **24a** and **25a** show a strong backbone curvature and in consequence, form amorphous films associated with relatively low charge carrier mobilities in the range of 10^{-3} $cm^2 V^{-1} s^{-1}$. Polymers **23b** and **25b** possess pseudo-straight-shaped backbones and yield ordered films with an edge-on orientation. Accordingly, **23b** and **25b** exhibit the highest mobilities within the series of 0.31 and 1.36 $cm^2 V^{-1} s^{-1}$, respectively. A lower mobility of **24b** in comparison to **23b** and **25b** was assigned to the stiff backbone which resulted in poor self-assembly and a low-ordered film (Fig. 17).[75]

Changes in the organization of D–A polymers related to differently shaped curvatures induced by additional thiophene units in the backbone have been reported for **26** and **27**.[57] Polymer **26** reveals a similar organization as observed for

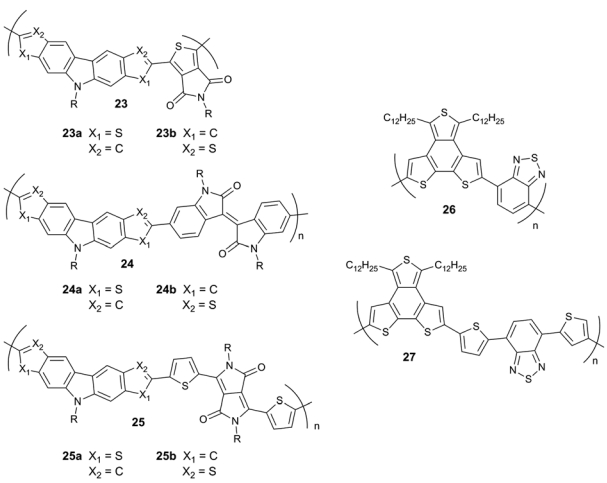

Fig. 17 Chemical structures of D–A polymers with different backbone curvatures influencing the organization.

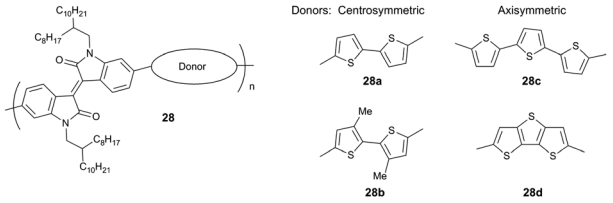

Fig. 18 Chemical structures of isoindigo-based polymers with centrosymmetric and axisymmetric donor units.

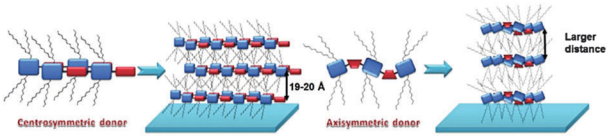

Fig. 19 Illustration of the film packings for **28** with centrosymmetric and axisymmetric donors. Reprinted with permission from ref. 54, Copyright 2012, American Chemical Society.

discotic columnar systems which is related to the disk-like shape of the donor unit packed on top of each other to form a columnar stack.[76] Additionally, **26** assembles in a face-on fashion on the substrate. In contrast, **27** organizes in edge-on oriented layers leading to a higher charge carrier mobility in transistors.[57] The strong backbone curvature in high mobility D–A polymers can be avoided by the right selection of the donor and acceptor units.[75] The role of the chemical structure of the donor unit on the backbone curvature has been described for centro- and axisymmetric units (Fig. 18).[54] Among these two systems, polymer **28a** with a centrosymmetric donor exhibits a low backbone curvature and therefore high crystallinity, improved lamellar packing and good interchain π-stacking leading to high a mobility around 1 $cm^2 V^{-1} s^{-1}$. Thereby, the packing is further favored by the "molecular docking" process described in Section 4.1 when the small unit docks into the cavity of the larger acceptor core (Fig. 6). Additional methyl groups at the donor lower the order of **28b** so that the mobility drops to 0.11 $cm^2 V^{-1} s^{-1}$ due to poor π-stacking interactions between polymer chains which nevertheless retain a linear backbone and a good lamellar packing. This value further decreases to 0.061 $cm^2 V^{-1} s^{-1}$ for **28c** and **28d** containing axisymmetric donors due to their higher backbone curvature which inhibits docking and reduces lamellar order (Fig. 19).

6. Conclusions

Conjugated D–A polymers provide a high degree of design freedom including the bulkiness of the substituents as well as structure factors like backbone curvature and molecular weight. Alkyl substituents ensure solubility which is required for the solution processing and microstructure formation in thin films. Additionally, substituents play an important role for the packing of the polymers and the backbone planarity. Higher steric demand of side chains which can arise from their geometry or from the substitution position at the backbone can significantly increase the π-stacking distance between conjugated backbones leading to a decrease in the hopping rate along the stacking direction. It is necessary to find the right balance between steric demand of the substituents, polymer packing and backbone twisting. Too bulky substituents provoke a backbone twist resulting in reduced order and lowered charge carrier migration along the conjugated polymer chain. Apparently, substituents seem to influence also the polymer surface arrangement in thin films. Depending on the type and position of the alkyls the organization can be switched between face-on and edge-on. The control over the surface arrangement is important for the implementation of polymers in electronic devices of different geometry.

Comprehensive understanding of the influence of chemical design of D–A polymers on their packing and assembly has been gained and is essential for the development of future high performance organic semiconductors. Identification of key conditions for a defect-free structure formation during solution processing allows a distinct control over the arrangement and orientation of D–A polymers on surfaces opening the door to novel large-scale roll-to-roll technologies.

Acknowledgements

This work was supported by the National Science Centre, Poland, through the grant UMO-2015/18/E/ST3/00322. We are grateful to Klaus Müllen and Wojciech Zajaczkowski for stimulating discussions.

Notes and references

1 Y. Ohmori, *Laser Photonics Rev.*, 2010, **4**, 300–310.
2 B. Geffroy, P. le Roy and C. Prat, *Polym. Int.*, 2006, **55**, 572–582.
3 R. A. Street, *Adv. Mater.*, 2009, **21**, 2007–2022.
4 H. Sirringhaus, *Adv. Mater.*, 2014, **26**, 1319–1335.
5 C. J. Brabec, N. S. Sariciftci and J. C. Hummelen, *Adv. Funct. Mater.*, 2001, **11**, 15–26.
6 S. Allard, M. Forster, B. Souharce, H. Thiem and U. Scherf, *Angew. Chem., Int. Ed.*, 2008, **47**, 4070–4098.
7 Z. Bao, *Adv. Mater.*, 2000, **12**, 227–230.
8 T. Sekitani, U. Zschieschang, H. Klauk and T. Someya, *Nat. Mater.*, 2010, **9**, 1015–1022.
9 D. J. Gundlach, *Nat. Mater.*, 2007, **6**, 173–174.
10 A. N. Sokolov, M. E. Roberts and Z. Bao, *Mater. Today*, 2009, **12**, 12–20.
11 S. Holliday, J. E. Donaghey and I. McCulloch, *Chem. Mater.*, 2014, **26**, 647–663.
12 P. M. Beaujuge and J. M. J. Fréchet, *J. Am. Chem. Soc.*, 2011, **133**, 20009–20029.
13 X. Guo, R. P. Ortiz, Y. Zheng, Y. Hu, Y.-Y. Noh, K.-J. Baeg, A. Facchetti and T. J. Marks, *J. Am. Chem. Soc.*, 2011, **133**, 1405–1418.
14 A. Facchetti, *Mater. Today*, 2007, **10**, 28–37.
15 G. M. Whitesides and M. Boncheva, *Proc. Natl. Acad. Sci. U. S. A.*, 2002, **99**, 4769–4774.
16 A. Mishra, C.-Q. Ma and P. Bäuerle, *Chem. Rev.*, 2009, **109**, 1141–1276.
17 T. Lei, Y. Cao, Y. Fan, C.-J. Liu, S.-C. Yuan and J. Pei, *J. Am. Chem. Soc.*, 2011, **133**, 6099–6101.
18 I. McCulloch, C. Bailey, M. Giles, M. Heeney, I. Love, M. Shkunov, D. Sparrowe and S. Tierney, *Chem. Mater.*, 2005, **17**, 1381–1385.
19 A. Facchetti, *Chem. Mater.*, 2011, **23**, 733–758.
20 A. Salleo, *Mater. Today*, 2007, **10**, 38–45.
21 R. Noriega, J. Rivnay, K. Vandewal, F. P. V. Koch, N. Stingelin, P. Smith, M. F. Toney and A. Salleo, *Nat. Mater.*, 2013, **12**, 1038–1044.
22 N.-K. Kim, S.-Y. Jang, G. Pace, M. Caironi, W.-T. Park, D. Khim, J. Kim, D.-Y. Kim and Y.-Y. Noh, *Chem. Mater.*, 2015, **27**, 8345–8353.
23 S. R. Forrest, *Nature*, 2004, **428**, 911–918.

24 H. N. Tsao and K. Müllen, *Chem. Soc. Rev.*, 2010, **39**, 2372–2386.
25 L. Biniek, B. C. Schroeder, C. B. Nielsen and I. McCulloch, *J. Mater. Chem.*, 2012, **22**, 14803–14813.
26 J. Peet, J. Y. Kim, N. E. Coates, W. L. Ma, D. Moses, A. J. Heeger and G. C. Bazan, *Nat. Mater.*, 2007, **6**, 497–500.
27 J. Y. Kim, K. Lee, N. E. Coates, D. Moses, T.-Q. Nguyen, M. Dante and A. J. Heeger, *Science*, 2007, **317**, 222–225.
28 J. S. Lee, S. K. Son, S. Song, H. Kim, D. R. Lee, K. Kim, M. J. Ko, D. H. Choi, B. Kim and J. H. Cho, *Chem. Mater.*, 2012, **24**, 1316–1323.
29 C. An, M. Li, T. Marszalek, D. Li, R. Berger, W. Pisula and M. Baumgarten, *Chem. Mater.*, 2014, **26**, 5923–5929.
30 Y. Liu, J. Zhao, Z. Li, C. Mu, W. Ma, H. Hu, K. Jiang, H. Lin, H. Ade and H. Yan, *Nat. Commun.*, 2014, **5**, 5293.
31 I. Kang, H.-J. Yun, D. S. Chung, S.-K. Kwon and Y.-H. Kim, *J. Am. Chem. Soc.*, 2013, **135**, 14896–14899.
32 B. Sun, W. Hong, Z. Yan, H. Aziz and Y. Li, *Adv. Mater.*, 2014, **26**, 2636–2642.
33 H. N. Tsao, D. M. Cho, I. Park, M. R. Hansen, A. Mavrinskiy, D. Y. Yoon, R. Graf, W. Pisula, H. W. Spiess and K. Müllen, *J. Am. Chem. Soc.*, 2011, **133**, 2605–2612.
34 M. Brinkmann, E. Gonthier, S. Bogen, K. Tremel, S. Ludwigs, M. Hufnagel and M. Sommer, *ACS Nano*, 2012, **6**, 10319–10326.
35 C. L. Donley, J. Zaumseil, J. W. Andreasen, M. M. Nielsen, H. Sirringhaus, R. H. Friend and J.-S. Kim, *J. Am. Chem. Soc.*, 2005, **127**, 12890–12899.
36 W. Zhang, J. Smith, S. E. Watkins, R. Gysel, M. McGehee, A. Salleo, J. Kirkpatrick, S. Ashraf, T. Anthopoulos, M. Heeney and I. McCulloch, *J. Am. Chem. Soc.*, 2010, **132**, 11437–11439.
37 T.-Y. Chu, J. Lu, S. Beaupré, Y. Zhang, J.-R. Pouliot, J. Zhou, A. Najari, M. Leclerc and Y. Tao, *Adv. Funct. Mater.*, 2012, **22**, 2345–2351.
38 X. Zhang, H. Bronstein, A. J. Kronemeijer, J. Smith, Y. Kim, R. J. Kline, L. J. Richter, T. D. Anthopoulos, H. Sirringhaus, K. Song, M. Heeney, W. Zhang, I. McCulloch and D. M. DeLongchamp, *Nat. Commun.*, 2013, **4**, 2238.
39 J. J. Intemann, K. Yao, H.-L. Yip, Y.-X. Xu, Y.-X. Li, P.-W. Liang, F.-Z. Ding, X. Li and A. K. Y. Jen, *Chem. Mater.*, 2013, **25**, 3188–3195.
40 B. Fu, J. Baltazar, Z. Hu, A.-T. Chien, S. Kumar, C. L. Henderson, D. M. Collard and E. Reichmanis, *Chem. Mater.*, 2012, **24**, 4123–4133.
41 H. N. Tsao, D. M. Cho, I. Park, M. R. Hansen, A. Mavrinskiy, Y. Yoon do, R. Graf, W. Pisula, H. W. Spiess and K. Müllen, *J. Am. Chem. Soc.*, 2011, **133**, 2605–2612.
42 Y. Li, P. Sonar, S. P. Singh, M. S. Soh, M. van Meurs and J. Tan, *J. Am. Chem. Soc.*, 2011, **133**, 2198–2204.
43 J. Li, Y. Zhao, H. S. Tan, Y. Guo, C.-A. Di, G. Yu, Y. Liu, M. Lin, S. H. Lim, Y. Zhou, H. Su and B. S. Ong, *Sci. Rep.*, 2012, **2**, 754.
44 J. Li, Y. Zhao, H. S. Tan, Y. Guo, C. A. Di, G. Yu, Y. Liu, M. Lin, S. H. Lim, Y. Zhou, H. Su and B. S. Ong, *Sci. Rep.*, 2012, **2**, 754.
45 I. Osaka, M. Akita, T. Koganezawa and K. Takimiya, *Chem. Mater.*, 2012, **24**, 1235–1243.
46 Y. Karpov, W. Zhao, I. Raguzin, T. Beryozkina, V. Bakulev, M. Al-Hussein, L. Häußler, M. Stamm, B. Voit, A. Facchetti, R. Tkachov and A. Kiriy, *ACS Appl. Mater. Interfaces*, 2015, **7**, 12478–12487.
47 J. Mei and Z. Bao, *Chem. Mater.*, 2014, **26**, 604–615.
48 D. M. DeLongchamp, R. J. Kline, E. K. Lin, D. A. Fischer, L. J. Richter, L. A. Lucas, M. Heeney, I. McCulloch and J. E. Northrup, *Adv. Mater.*, 2007, **19**, 833–837.
49 I. Osaka, R. Zhang, G. Sauvé, D.-M. Smilgies, T. Kowalewski and R. D. McCullough, *J. Am. Chem. Soc.*, 2009, **131**, 2521–2529.
50 V. Coropceanu, J. Cornil, D. A. da Silva Filho, Y. Olivier, R. Silbey and J.-L. Brédas, *Chem. Rev.*, 2007, **107**, 926–952.
51 W. Pisula, H. Tsao, D. Dudenko, D. Cho, S. Puniredd, Y. Zhao, A. Mavrinskiy, J. Shu, M. Hansen, M. Baumgarten and K. Müllen, *Polymers*, 2013, **5**, 833.
52 Y. Olivier, D. Niedzialek, V. Lemaur, W. Pisula, K. Müllen, U. Koldemir, J. R. Reynolds, R. Lazzaroni, J. Cornil and D. Beljonne, *Adv. Mater.*, 2014, **26**, 2119–2136.
53 A. T. Yiu, P. M. Beaujuge, O. P. Lee, C. H. Woo, M. F. Toney and J. M. J. Fréchet, *J. Am. Chem. Soc.*, 2012, **134**, 2180–2185.
54 T. Lei, Y. Cao, X. Zhou, Y. Peng, J. Bian and J. Pei, *Chem. Mater.*, 2012, **24**, 1762–1770.
55 J. Guo, Y. Liang, J. Szarko, B. Lee, H. J. Son, B. S. Rolczynski, L. Yu and L. X. Chen, *J. Phys. Chem. B*, 2010, **114**, 742–748.
56 F. C. Grozema, P. T. van Duijnen, Y. A. Berlin, M. A. Ratner and L. D. A. Siebbeles, *J. Phys. Chem. B*, 2002, **106**, 7791–7795.
57 X. Guo, S. R. Puniredd, M. Baumgarten, W. Pisula and K. Müllen, *Adv. Mater.*, 2013, **25**, 5467–5472.
58 C. Cabanetos, A. El Labban, J. A. Bartelt, J. D. Douglas, W. R. Mateker, J. M. Frechet, M. D. McGehee and P. M. Beaujuge, *J. Am. Chem. Soc.*, 2013, **135**, 4656–4659.
59 S. Nishinaga, H. Mori and Y. Nishihara, *Macromolecules*, 2015, **48**, 2875–2885.
60 I. Osaka, M. Saito, T. Koganezawa and K. Takimiya, *Adv. Mater.*, 2014, **26**, 331–338.
61 J. Lee, A. R. Han, J. Kim, Y. Kim, J. H. Oh and C. Yang, *J. Am. Chem. Soc.*, 2012, **134**, 20713–20721.
62 J. Lee, A. R. Han, H. Yu, T. J. Shin, C. Yang and J. H. Oh, *J. Am. Chem. Soc.*, 2013, **135**, 9540–9547.
63 T. Lei, J. H. Dou and J. Pei, *Adv. Mater.*, 2012, **24**, 6457–6461.
64 J. Lee, T. Marszalek, K. C. Lee, J. Kim, W. Pisula and C. Yang, *Macromol. Chem. Phys.*, 2015, **216**, 1244–1250.
65 H. Chen, Y. Guo, G. Yu, Y. Zhao, J. Zhang, D. Gao, H. Liu and Y. Liu, *Adv. Mater.*, 2012, **24**, 4618–4622.
66 S. Chen, B. Sun, W. Hong, H. Aziz, Y. Meng and Y. Li, *J. Mater. Chem. C*, 2014, **2**, 2183.
67 J. Mei, H. Kim do, A. L. Ayzner, M. F. Toney and Z. Bao, *J. Am. Chem. Soc.*, 2011, **133**, 20130–20133.
68 J. Lee, A. R. Han, H. Yu, T. J. Shin, C. Yang and J. H. Oh, *J. Am. Chem. Soc.*, 2013, **135**, 9540–9547.
69 J. Y. Back, H. Yu, I. Song, I. Kang, H. Ahn, T. J. Shin, S.-K. Kwon, J. H. Oh and Y.-H. Kim, *Chem. Mater.*, 2015, **27**, 1732–1739.
70 Q. Wu, M. Wang, X. Qiao, Y. Xiong, Y. Huang, X. Gao and H. Li, *Macromolecules*, 2013, **46**, 3887–3894.
71 M. Kuhn, J. Ludwig, T. Marszalek, T. Adermann, W. Pisula, K. Müllen, A. Colsmann and M. Hamburger, *Chem. Mater.*, 2015, **27**, 2678–2686.
72 C. Liu, S. Dong, P. Cai, P. Liu, S. Liu, J. Chen, F. Liu, L. Ying, T. P. Russell, F. Huang and Y. Cao, *ACS Appl. Mater. Interfaces*, 2015, **7**, 9038–9051.
73 J. Lee, A. R. Han, J. Hong, J. H. Seo, J. H. Oh and C. Yang, *Adv. Funct. Mater.*, 2012, **22**, 4128–4138.
74 R. Rieger, D. Beckmann, A. Mavrinskiy, M. Kastler and K. Müllen, *Chem. Mater.*, 2010, **22**, 5314–5318.
75 Y. Deng, Y. Chen, X. Zhang, H. Tian, C. Bao, D. Yan, Y. Geng and F. Wang, *Macromolecules*, 2012, **45**, 8621–8627.
76 W. Pisula, X. A. Feng and K. Müllen, *Adv. Mater.*, 2010, **22**, 3634–3649.